Use of a purified and functional recombinant calcium-channel β_4 subunit in surface-plasmon resonance studies

Sandrine GEIB*, Guillaume SANDOZ*, Kamel MABROUK†, Alessandra MATAVEL*, Pascale MARCHOT†, Toshinori HOSHI‡, Michel VILLAZ*, Michel RONJAT*, Raymond MIQUELIS†§, Christian LÉVÊQUE§‖ and Michel DE WAARD*[1]

*INSERM EMI 99-31, Canaux Ioniques et Signalisation, CEA, DBMS, 17, rue des Martyrs, 38054 Grenoble Cedex 9, France, †CNRS UMR 6560, Laboratoire de Biochimie, boulevard Pierre Dramard, 13916 Marseille Cedex 20, France, ‡Department of Physiology, 3700 Hamilton Walk, University of Pennsylvania, Philadelphia, PA 19104, U.S.A., §Unité de Méthodologie des Interactions Moléculaires (UNIM), IFR Jean Roche, boulevard Pierre Dramard, 13916 Marseille Cedex 20, France, and ‖INSERM U464, Laboratoire Neurobiologie des Canaux Ioniques, IFR Jean Roche, boulevard Pierre Dramard, 13916 Marseille Cedex 20, France

Native high-voltage-gated calcium channels are multi-subunit complexes comprising a pore-forming subunit Ca_v and at least two auxiliary subunits $\alpha_2\delta$ and β. The β subunit facilitates cell-surface expression of the channel and contributes significantly to its biophysical properties. In spite of its importance, detailed structural and functional studies are hampered by the limited availability of native β subunit. Here, we report the purification of a recombinant calcium-channel β_4 subunit from bacterial extracts by using a polyhistidine tag. The purified protein is fully functional since it binds on the alpha1 interaction domain, its main Ca_v-binding site, and regulates the activity of P/Q calcium channel expressed in *Xenopus* oocytes in a similar way to the β_4 subunit produced by cRNA injection. We took advantage of the functionality of the purified material to (i) develop an efficient surface-plasmon resonance assay of the interaction between two calcium channel subunits and (ii) measure, for the first time, the affinity of the recombinant His-β_4 subunit for the full-length $Ca_v2.1$ channel. The availability of this purified material and the development of a surface-plasmon resonance assay opens two immediate research perspectives: (i) drug screening programmes applied to the Ca_v/β interaction and (ii) crystallographic studies of the calcium-channel β_4 subunit.

Key words: auxiliary subunit, heterologous expression, *Xenopus* oocyte.

INTRODUCTION

Voltage-dependent calcium channels are crucial to the homoeostasis of calcium in excitable cells by tightly regulating calcium influx into the cytosol. These channels are involved in a large variety of intracellular functions including the control of electrical excitability, metabolism, gene expression [1], vesicle release [2], cell differentiation and neuronal growth. Several classes of voltage-dependent calcium channels have been identified and classified according to pharmacological, biophysical and molecular properties [3]. Low-voltage-activated calcium channels (Ca_v3 class) differ from high-voltage-dependent calcium channels (Ca_v1 and Ca_v2 classes) by their subunit composition. A consensus view on high-voltage-activated calcium channels is that at least two auxiliary subunits are associated with the main Ca_v pore subunit: an integral membrane protein called $\alpha_2\delta$, which is highly glycosylated, and a protein that is entirely localized in the cytoplasm termed β. So far, three genes code for different but highly homologous $\alpha_2\delta$ subunits and four genes for the β subunit (β_1 to β_4). The importance of these subunits in channel properties and function has been clearly highlighted by heterologous expression [4,5], antisense [6] and gene knock-out experiments [7]. For the β-subunit function, at least, this protein is required for a normal cell-surface expression of these channels [8] and for normalizing the kinetic and voltage dependence of calcium influx (see [9] for a review). Besides, there is also evidence that it may play a role in a differential distribution of voltage-dependent calcium channels at the cell surface [10]. Finally, knock-out of the β_1-subunit gene leads to a lack of excitation–contraction coupling in skeletal muscles [7]. Also, the cytoplasmic localization of the β subunit strongly suggests that it represents an ideal target for ion-channel regulation by kinases and phosphates, and for establishing molecular interactions of the channel with intracellular proteins required for calcium-channel function and/or localization [11].

In spite of the importance of the auxiliary β subunit in channel assembly and function, little is known about the structure of these proteins. A recent modelling study on the β_{1b} subunit by Hanlon and co-workers [12] suggests the presence of a functional Src homology 3 domain, an N-terminal sequence similar to a PDZ domain and a structure related to the membrane-associated guanylate-kinase protein family. Strong amino-acid sequence homologies among various β-subunit isoforms, in domains that are not suspected to interact with Ca_v regions, are also indicative that β subunits represent an interface at which proteins external to the calcium-channel complex can interact. This evidence clearly implies that a better knowledge of the three-dimensional structure of the β subunits would considerably ease the understanding of the intracellular functions of this essential channel protein. Purification of a functional recombinant β subunit has been hindered by various problems since the structure of this subunit appears to be highly sensitive to this type of construct. For instance, the addition of a green-fluorescent-protein tag to a β subunit misleads the protein to the nucleus. Also, purified glutathione S-transferase (GST)-tagged β subunits are unable to bind to the alpha1 interaction domain (AID), a β-subunit-anchoring sequence present in each class of Ca_v1 and Ca_v2 channels (M. De Waard and K. P. Campbell, unpublished work).

Abbreviations used: AID, alpha1 interaction domain; β_{4RNA}, β_4 expressed by cRNA injection; GST, glutathione S-transferase; MCAC, metal-chelate affinity chromatography; SPR, surface-plasmon resonance.

[1] To whom correspondence should be addressed (e-mail mdewaard@cea.fr).

In this study, we demonstrate that the β subunit can be purified successfully with the help of a recombinant polyhistidine tag. We focused on the purification of the β_4 subunit for various reasons. First, the β_4 subunit is of relevant physiological interest since mutations in the *CACNB4* gene produce various neurological disorders in lethargic (lh) mice [13] and humans suffering from idiopathic generalized epilepsy and episodic ataxia [14]. Secondly, contrary to other β isoforms, such as β_{1b} or β_2 [15,16], β_4 does not associate with the membrane. Our purified β_4 protein remains functional both for binding on to AID in surface-plasmon resonance (SPR) experiments and for ion-channel regulation after injection into *Xenopus* oocytes. Finally, we efficiently used the purified protein to determine the first *in situ* binding affinity of β_4 subunit on to the full-length $Ca_v2.1$ channel.

EXPERIMENTAL

cDNA constructions

The full-length rat β_4 cDNA (GenBank® no. L02315) was amplified by PCR with the following primers: 5′-CATGCCATGGCAATGTCGTCCTCCTACGCCAAGAACGGGGCG-3′ (forward) and 5′-GCTCTAGAGTCAAAGCCTATGTCGGGAGTCATGGCTGCATCC-3′ (reverse) containing *Nco*I and *Xba*I restriction sites, respectively. The PCR product was subcloned into the *Nco*I and *Xba*I sites of pMR78 [17]. This vector encodes a His tag that is located 5′ to the β_4 sequence.

Purification of the recombinant rat His-β_4 protein

Large BL21 star bacteria (InVitrogen) cultures (400 ml), transformed with the pMR78-His-β_4 plasmid were grown at 23 °C under agitation until a D_{600} of 0.8 was reached. Protein synthesis was induced by the addition of 1 mM isopropyl β-D-galactopyranoside (Sigma) to the culture media for 4 h. The bacteria were then pelleted (3000 ***g*** for 10 min on a Centrikon A 6.14 rotor; Kontron Instruments, Watford, Herts., U.K.) at 4 °C and resuspended in 5 ml metal-chelate affinity chromatography (MCAC) buffer without imidazole [MCAC-0; composition: 20 mM Tris/HCl, 500 mM NaCl, 10 % (v/v) glycerol, pH 8.0) supplemented with 0.23 mM PMSF and a cocktail of protease inhibitors (Complete™, Boehringer, Mannheim, Germany)]. After adding Triton X-100 to a final concentration of 0.1 % (v/v), the suspension was subjected to 3 cycles of freezing and thawing on ice. The following components were then added to the suspension: 1 mg lysosyme/ml, 10 μg DNAse I/ml and 10 mM $MgCl_2$, and the mixture was incubated for 10 min at room temperature (20–22 °C). The cell lysate was centrifuged for 15 min at 20000 ***g*** (4 °C). The supernatant was kept on ice. Iminodiacetic acid (5 ml) coupled with Sepharose beads (Sigma) was added to a disposable polypropylene column, with a final bed volume of 2 ml. The column was washed with 5 vols. of water, charged with 5 vols. of $NiSO_4$ (50 mM) and equilibrated with 2 ml MCAC-0 buffer. The sample was then applied on to the column and washed with 20 ml MCAC-60 buffer (MCAC-0 supplemented with 60 mM imidazole). The elution was performed with 6 ml MCAC-200 elution buffer (MCAC-0 supplemented with 200 mM imidazole). Fractions of 1 ml were collected during elution. The protein concentration of each fraction was determined by a Bradford assay using commercial reagents (Pierce). Fractions were analysed by SDS/PAGE (9–15 % gel) and protein bands were visualized by staining with Coomassie Blue. The most concentrated fractions of His-β_4 were kept at 4 °C and used rapidly for the experiments. Purified His-β_4 conserved at this temperature appeared functionally stable for weeks.

Purification of GST and GST-$AID_{2.1}$ fusion proteins

The GST-$AID_{2.1}$ fusion protein (formerly termed GST-AID_A) is encoded by a pGEX2T vector as described previously [18]. It contains the rabbit $Ca_v2.1$ sequence from amino-acid residues 369–418 [19]. Both GST and GST-$AID_{2.1}$ fusion proteins were purified according to procedures described by De Waard and coworkers [20].

Western-blot detection

Proteins from non-induced and induced BL21 star bacteria and purified His-β_4 protein were separated by SDS/PAGE (9 % gel) and transferred on to a nitrocellulose membrane (Hybond ECL®, Amersham, Bucks., U.K.) as previously described [21]. Protein detection with the monoclonal anti-His antibody was performed according to the procedures of the manufacturer (Qiagen).

In vitro binding of His-β_4 to GST or GST-$AID_{2.1}$

To test the proportion of active His-β_4, 7.5 μg of purified material was incubated in TBS, Triton X-100 [0.1 %, v/v] with GST or GST-$AID_{2.1}$ coupled with glutathione agarose beads at concentrations defined in the text. The reaction volume was 100 μl. After 4 h incubation, the pellet was washed with 50 μl Tris-buffered saline, Triton X-100 (0.1 %). Both the supernatant and the first wash were pooled and kept for analysis (120 μl). Three other washing steps were performed with 1 ml buffer, and discarded. The various pellets and supernatants were then analysed by SDS/PAGE (9 % gel) and bands were revealed by Coomassie Blue staining.

Protein-binding experiments by SPR

Binding experiments and kinetic analysis were performed at 25 °C using a Biacore 3000 Instrument (Uppsala, Sweden). The sensor chips (CM5, Biacore AB) were chemically activated by the injection of 35 μl of a 1:1 mixture of *N*-hydroxysuccinimide (50 mM) and *N*-ethyl-*N*′-(3-dimethylaminopropyl)carbodi-imide (200 mM) at a flow rate of 5 μl/min. The chemical modification enables the carboxymethylated dextran matrix to bind the free amino groups of proteins covalently. Polyclonal goat anti-GST antibodies (Pharmacia) solubilized in acetate buffer (pH 4.8) were applied to the matrix according to the manufacturer's instructions. The remaining matrix sites, which did not react with the anti-GST antibodies, were blocked by the injection of 35 μl of 1 M ethanolamine solution. The amount of anti-GST antibodies immobilized corresponds to approx. 10000 resonance units. Next, 7.5–15 fmol GST or GST-$AID_{2.1}$ was captured by the anti-GST antibodies. For binding studies, a range of purified His-β_4 protein (from 1 to 300 nM) was injected in both control GST and GST-$AID_{2.1}$ flow cells at a rate of 20 μl/min. Non-specific binding amounted to 8–14 %. The dissociation data were collected over a time span of 500 s. His-β_4 dilution and running buffers were identical and contained 200 mM NaCl, 8 mM imidazole, 4 mM spermine, 12 mM Tris/HCl, 1 % (v/v) glycerol and 0.1 % (v/v) Triton X-100, pH 7.4. The surface of the sensor chip, with its coated anti-GST antibodies, was regenerated by injecting 10 μl of 0.1 M glycine (pH 2.2).

For data analysis, rate constants were calculated by global fitting [22] using the BIA 3.0 evaluation program (Biacore AB). The observed data were fitted to a single-site interaction model. The analysis software corrects for the systematic drift in the baseline that occurred during measurements. The quality of the fit was assessed by inspecting the statistical χ^2 value and

the residuals (observed − calculated). The χ^2 values were in the range of 1.5–20, and the residuals, randomly distributed, did not exceed ± 1–8% of the experimental curves. To confirm the absence of a mass-transport effect, we checked that the rate constants remained unchanged by using a higher flow rate of His-β_4 over GST-AID$_{2.1}$ (75 μl/min).

Xenopus laevis oocyte injection

Stage V and VI *X. laevis* oocytes were collected, maintained and injected with cRNA as described previously [23,24]. Purified His-β_4 protein concentration was as defined earlier. Electrophysiological recordings were performed 5–9 days after cRNA or cRNA/His-β_4 injection.

Electrophysiological recordings and data analysis

Oocyte currents were recorded at room temperature (20–22 °C) as described previously [23]. The results were presented as the means ± S.E.

RESULTS AND DISCUSSION

Purification of an N-terminal polyhistidine-tagged β_4 subunit

For the purification of the rat β_4 subunit, we subcloned the cDNA sequence into the pMR78 vector kindly provided by Dr Cheynet [17]. This vector plays an important role in recombinant protein purification because it contains a minicistron for high-level expression and a sequence coding for a polyhistidine tail, which is positioned at the 5′-terminal end of the β_4 cDNA sequence. We have tested several purification protocols, all including sonication as a procedure for bacterial lyses, and found that most yielded pure but non-functional proteins (results not shown). Therefore we proceeded to an optimization of the purification procedures by adapting bacterial growth, protein synthesis induction, cell lysis and buffer conditions. We found that a growth temperature of 23 °C and an OD_{600} of 0.8 were the optimal conditions for increasing protein yield. We also modified the buffer composition for column washing and protein elution, essentially by adding glycerol and by increasing ionic strength. These conditions favoured solubility and contributed to a better folding of the purified protein according to our testing. Figure 1 shows the various steps used for the purification of His-β_4 protein. The Coomassie Blue-stained gel illustrates that His-β_4 remains a minor component after induction compared with the protein content of the bacterial lysate. Although His-β_4 protein is present in limited amounts as a soluble fraction in bacteria, the degree of purity of His-β_4 after elution is high. The purified protein has a molecular mass of approx. 58 kDa, which is in agreement with the theoretical expectations (59 kDa). The identity of the protein was validated by Western blot with a monoclonal anti-polyhistidine antibody (Figure 1B). Protein concentration in the most concentrated elution fraction varied between 0.2 and 0.6 mg/ml as determined by a Bradford assay ($n = 10$ purifications). The total quantity of purified His-β_4 amounted to approx. 0.6–4 mg on average per assay (400 ml

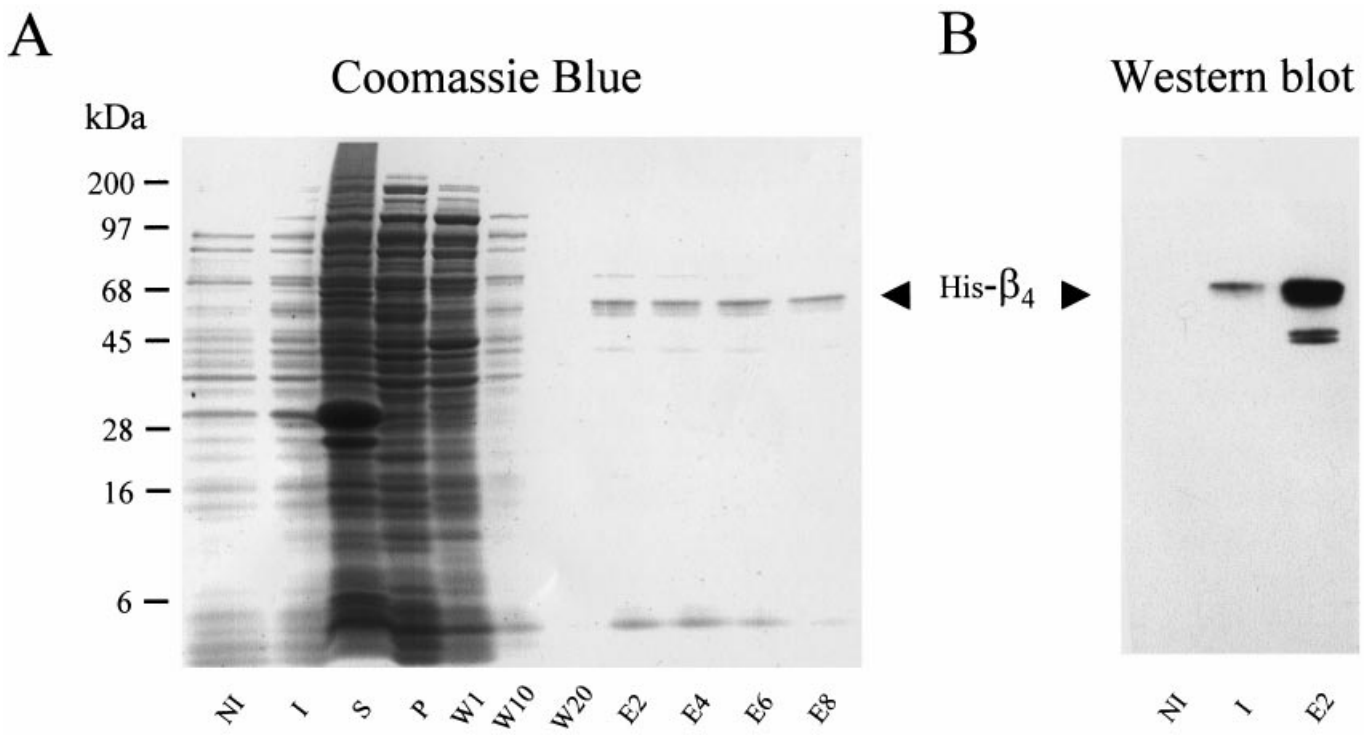

Figure 1 Purification of the rat His-β_4 protein

(**A**) Coomassie Blue staining by SDS/PAGE (9–15% gradient) illustrating the various steps of His-β_4 purification. Lane 1, crude lysate (100 μl) of non-induced (NI) *Escherichia coli* BL21 star cells transformed with pMR78-β_4-His vector; lane 2, crude lysate (50 μl) of induced (I) BL21 star cells; lanes 3 and 4, supernatant (S) and pellet (P), respectively after cell lysis and centrifugation of the bacterial suspension (10 and 3 μl, respectively); lanes 5–7, 10 μl of the 1st, 10th and 20th ml column wash with loading buffer (W1, W10 and W20, respectively); lanes 8–12, 10 μl of 1 ml elution fractions 2, 4, 6 and 8 (E2, E4, E6 and E8). (**B**) Western blot of non-induced BL21 bacteria, induced bacteria and 4 μg of the purified protein (elution fraction 2) with anti-His.

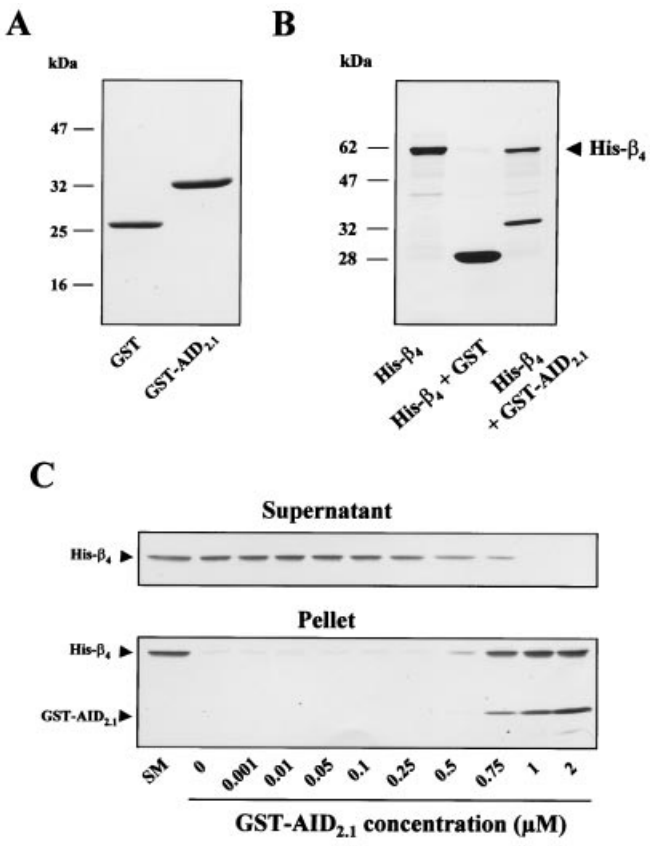

Figure 2 Binding properties of rat His-β_4 on GST-AID$_{2.1}$ fusion protein

(**A**) Coomassie Blue staining by SDS/PAGE (9% gel) illustrating the purified GST and GST-AID$_{2.1}$ fusion proteins used for SPR experiments. (**B**) Binding of purified His-β_4 (4 μM) on GST (10 μM) or GST-AID$_{2.1}$ (2 μM). Glutathione agarose beads were used to immobilize GST or GST-AID$_{2.1}$. A 2-fold excess molar fraction of His-β_4 over GST-AID$_{2.1}$ was used to enhance the fraction of structurally active purified His-β_4 protein. The concentration of GST was five times higher than GST-AID$_{2.1}$ to demonstrate that non-specific binding is negligible in our binding conditions. The stoichiometry of the His-β_4/GST-AID$_{2.1}$ binding appears close to 1:1. (**C**) Coomassie Blue-stained polyacrylamide gels showing the proportion of active His-β_4 protein. Top panel, analysis of the supernatants obtained after incubation with increasing amounts of GST-AID$_{2.1}$ protein. Bottom panel, analysis of the pellets obtained under the same conditions. SM, starting material; 0, glutathione beads alone. Full depletion of His-β_4 was reached at fusion protein concentrations above 0.75 μM.

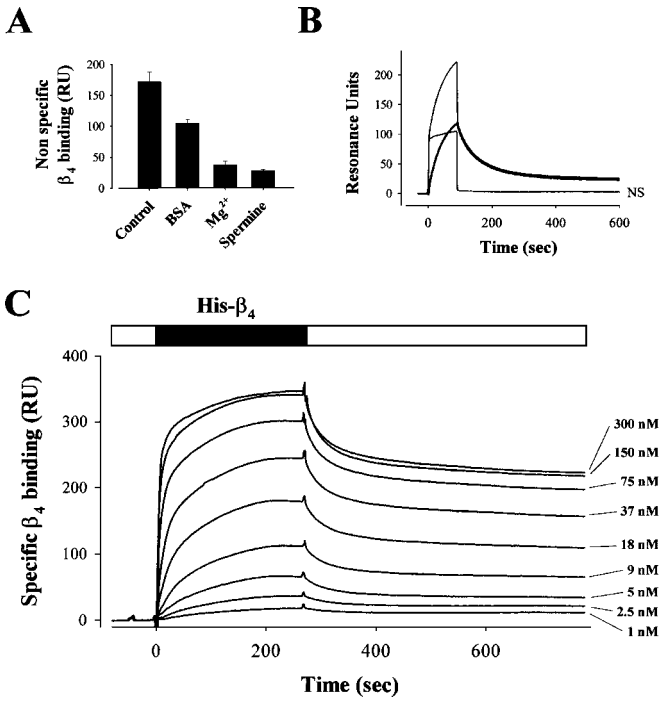

Figure 3 Development of an SPR technique for the main Ca$_v$/β interaction

(**A**) Average effect of positively charged molecules on the non-specific binding of purified His-β_4 on GST protein. The running buffer used contained 50 mM Tris, 150 mM NaCl and 0.1% Triton X-100. A channel loaded with anti-GST antibodies was injected with running buffer containing 16 nM of purified His-β_4 alone (Control) or in combination with 0.5% BSA (BSA), 40 mM $MgCl_2$ (Mg^{2+}) or 4 mM spermine (Spermine). RU, resonance units. (**B**) SPR measurements of 16 nM His-β_4 interaction with GST [bulk + non-specific (NS)] or GST-AID$_{2.1}$ (Total). The specific His-β_4 binding is also illustrated (thick line) by subtraction of the two traces [Total — (bulk + NS)]. (**C**) Specific interaction of His-β_4 (shown at various concentrations) with GST-AID$_{2.1}$ immobilized on the surface of the matrix. Open bars, control running buffer; filled bar, His-β_4 injection. The last two concentrations of His-β_4 (150 and 300 nM) show the saturation of the binding. Maximum His-β_4 binding, 344 RU for 240 RU of GST-AID$_{2.1}$ immobilized on the chip. This results in an RU ratio of 1.43 which should be compared with the molecular mass ratio of 58:37 of 1.56. The amount of active GST-AID$_{2.1}$ would then correspond to 90% assuming that 100% of His-β_4 proteins are active.

culture, 4 h induction). The most concentrated protein fractions were kept at 4 °C for immediate use in binding (Figures 2 and 3) and expression experiments (Figures 4–6). We next tested whether the purified His-β_4 subunit was properly folded according to some current evaluation criteria. In particular, we examined the ability of the protein to bind to a high-threshold Ca$_v$ channel and regulate calcium-channel activity.

Purified His-β_4 efficiently recognizes its main Ca$_v$-binding site

Calcium-channel β subunits are able to bind to both the Ca$_v$1 and Ca$_v$2 classes of calcium channels [18,20,25]. This binding occurs at a well-defined site localized in the cytoplasmic I–II loop of these channels and termed AID. In the present study, we evaluated whether the purified His-β_4 had an active conformation for interacting with the AID sequence of the P/Q calcium channel (AID$_{2.1}$). A Coomassie Blue stained SDS/polyacrylamide (9%) gel illustrates the fusion proteins (control GST or GST-AID$_{2.1}$), purified according to standard procedures [20], which were used in His-β_4-binding experiments (Figure 2A). Next, these fusion proteins were coupled with glutathione beads, and the ability of these beads to bind purified His-β_4 proteins was determined. In agreement with earlier findings, we found that only beads on to which GST-AID$_{2.1}$ was immobilized have the ability to bind purified His-β_4 protein (Figure 2B). No binding was observed on glutathione beads alone (Figure 2C) or on to control GST glutathione beads (Figure 2B). We next evaluated whether increasing concentrations of GST-AID$_{2.1}$ could successfully deplete the initial His-β_4 material present in the supernatant. Figure 2(C) demonstrates that full depletion of His-β_4 could occur at saturating concentrations of GST-AID$_{2.1}$. This was also shown by the concomitant increase in His-β_4 associated with GST-AID$_{2.1}$ beads in the pellet. These results suggest that, in our preparation, most purified His-β_4 molecules are in an active conformation for AID binding.

Amongst the various approaches used to evaluate the interaction between the β subunit and AID, overlay techniques have been used for a qualitative description [18], whereas GST fusion protein immobilization on to glutathione beads appeared effective for quantitative information [20]. These approaches are

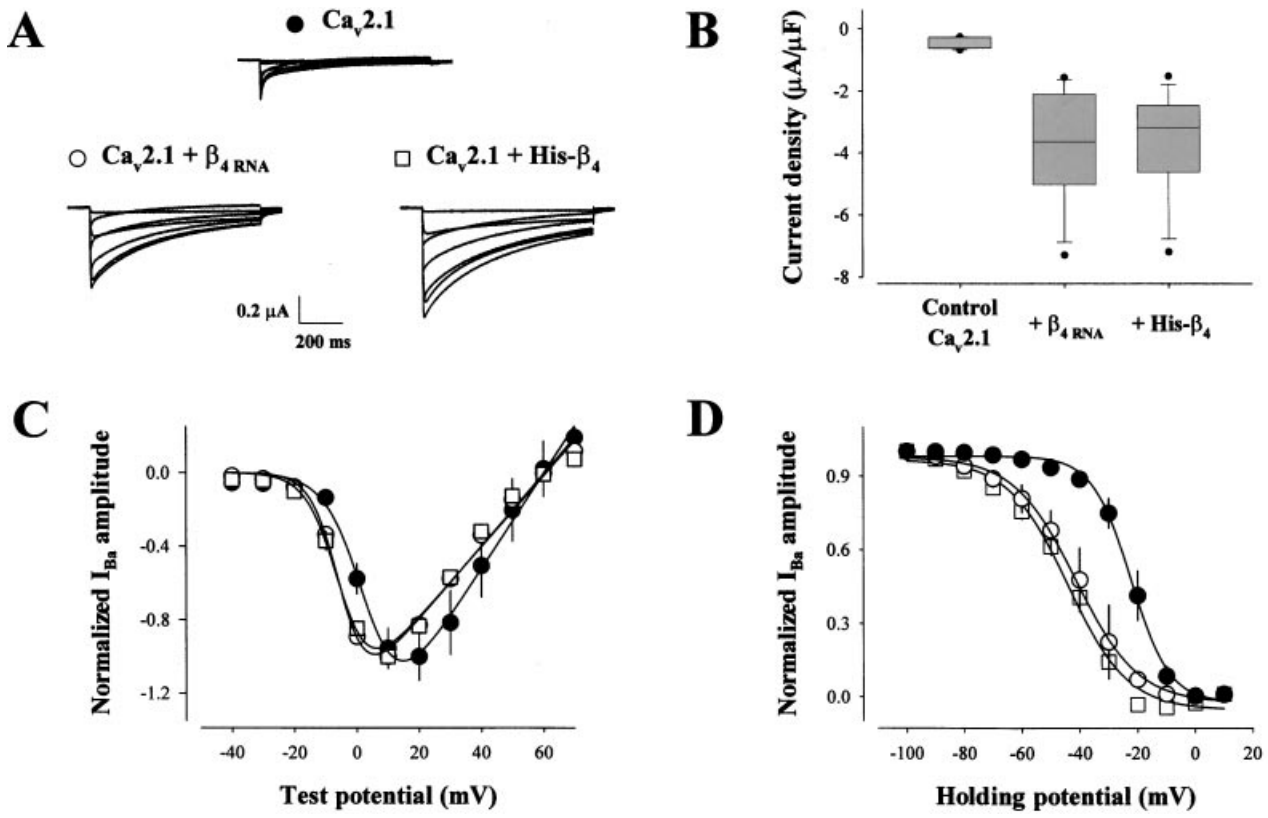

Figure 4 The purified His-β_4 protein is fully functional for calcium-channel regulation

(**A**) Representative current traces of $Ca_v2.1$ channel expressed in *Xenopus* oocytes alone (top) or in combination with β_4 cRNA (left) or purified His-β_4 protein (right). Purified His-β_4 was co-injected with $Ca_v2.1$ cRNA at a concentration of 5 nM. Holding potential was −90 mV and currents were evoked by membrane depolarization to −20, −10, 0, 10, 20, 30 and 40 mV. (**B**) Average Ba^{2+} current densities measured at a membrane depolarization of 20 mV for $Ca_v2.1$ ($n = 7$), $Ca_v2.1/\beta_{4\,RNA}$ ($n = 7$) and $Ca_v2.1$/His-β_4 ($n = 9$) channels. Box plot representation. (**C**) Average normalized current−voltage relation for $Ca_v2.1$ (●, $n = 19$), $Ca_v2.1/\beta_{4\,RNA}$ (○, $n = 7$) and $Ca_v2.1$/His-β_4 (□, $n = 11$) channels. Both β_4 cRNA and His-β_4 protein produced a leftward shift in the voltage dependence. Fits of *I–V* curves were obtained assuming an activation curve of the Boltzmann type:

$$I_{Ba} = [g(V - E)]/[1 + \exp(-(V - V_{\frac{1}{2}}/k))].$$

The results yield normalized conductances of $g = -0.026 \pm 0.001$ ($Ca_v2.1$), -0.019 ± 0.001 ($Ca_v2.1/\beta_{4\,RNA}$) and -0.019 ± 0.001 ($Ca_v2.1$/His-β_4), half-activation potentials of -5.0 ± 0.81 mV ($Ca_v2.1/\beta_{4\,RNA}$) and -5.1 ± 1.3 mV ($Ca_v2.1$/His-β_4), slopes of $k = 6.0 \pm 0.4$ mV ($Ca_v2.1$), 4.5 ± 5.6 mV ($Ca_v2.1/\beta_{4\,RNA}$) and 5.1 ± 0.9 mV ($Ca_v2.1$/His-β_4), and reversal potentials of $E = 60.2 \pm 0.6$ mV ($Ca_v2.1$), 60.4 ± 1.3 mV ($Ca_v2.1/\beta_{4\,RNA}$) and 60.9 ± 1.9 mV ($Ca_v2.1$/His-β_4). (**D**) Average normalized steady-state inactivation curves for $Ca_v2.1$ (●, $n = 3$), $Ca_v2.1/\beta_{4\,RNA}$ (○, $n = 12$) and $Ca_v2.1$/His-β_4 (□, $n = 7$) channels. Peak current amplitudes are normalized to the maximum current reached during stimulation and plotted as a function of holding potential. Inter-pulse time was 30 s and test depolarization was 20 mV. Steady-state inactivation curves were also described by the Boltzmann equation

$$I_{Ba} = \{1 + \exp[(V - V_{\frac{1}{2}})/k]\}$$

Fits to the data yield half-inactivation potentials of $V_{\frac{1}{2}} = -22.3 \pm 0.7$ mV ($Ca_v2.1$), -41.3 ± 0.9 mV ($Ca_v2.1/\beta_{4\,RNA}$) or -44.1 ± 1.6 mV ($Ca_v2.1$/His-β_4) and slopes of $k = -6.7 \pm 0.6$ mV ($Ca_v2.1$), -10.6 ± 0.8 mV ($Ca_v2.1/\beta_{4\,RNA}$) or -10.3 ± 1.4 mV ($Ca_v2.1$/His-β_4).

useful to detect the interaction or to assess the binding affinity *in vitro* (found to be in the low nm, range with *in vitro*-translated β subunits). However, none of these techniques is very useful for large-scale drug-screening tests or kinetic analyses; hence alternative approaches should be developed. Recent studies [26,27] suggest that the SPR technique is more effective for a pharmacological-screening approach.

Development of an SPR technique to evaluate the interaction between His-β_4 and the AID sequence

The purification of His-β_4 represents a unique opportunity to develop this interaction technique for the Ca_v/β interaction and to determine the association and dissociation constants. Therefore we chose a CM5 carboxymethylated dextran matrix on which we could covalently immobilize anti-GST antibodies (see the Experimental section). Figure 3(A) demonstrates that purified His-β_4 produces a strong non-specific interaction with the matrix/antibody surface. We thus evaluated the buffer conditions required to lower this non-specific interaction to its minimum possible level. We found that if 0.5% BSA was added to the running buffer, there was only a 39 ± 3% decrease in the non-specific interaction of His-β_4 with the matrix (Figure 3A). More drastic decreases in non-specific His-β_4 association were obtained if Mg^{2+} (40 mM) or spermine (4 mM) was included in the running buffer. The average decrease in non-specific association amounted to 78 ± 3% (Mg^{2+}) and 84 ± 1% (spermine). Translated into total resonance units, the non-specific interaction equalled 28 ± 2 resonance units for spermine addition. The requirement for positively charged molecules (Mg^{2+}) to lower non-specific His-β_4 binding probably reflects an interaction of His-β_4 with the remaining free carboxylic groups at the surface of the matrix. The effect of spermine can also be interpreted similarly owing to its basic properties. Similar conclusions were reached if

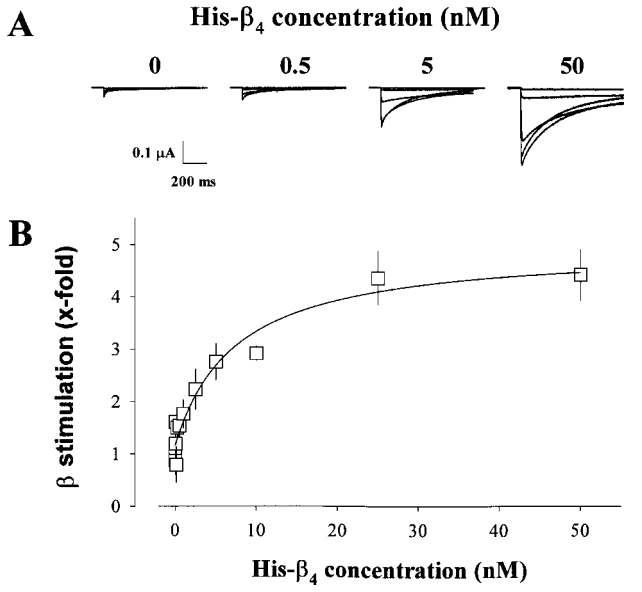

Figure 5 His-β_4 concentration dependence of $Ca_v2.1$ expression stimulation

(**A**) Representative current traces at −20, −10, 0, 10 and 20 mV for $Ca_v2.1$ alone or $Ca_v2.1$ co-injected with various His-β_4 protein concentrations. Time of expression was 6–7 days. (**B**) Concentration dependence of the His-β_4 effect on the increase in $Ca_v2.1$ current density. Peak current amplitudes were determined for a membrane depolarization of 20 mV and current densities were calculated based on the individual cell-membrane capacitance. The average current density stimulation was produced by His-β_4. The data were fitted to a hyperbolic function $y = y_0 + (ax)/(EC_{50} + x)$ where x is the His-β_4 concentration, $y_0 = 1.1 \pm 0.1$ is the basal stimulation factor in the absence of His-β_4, $a = 3.8 \pm 0.4$, the maximal stimulation factor and $EC_{50} = 7.4 \pm 2.5$ nM.

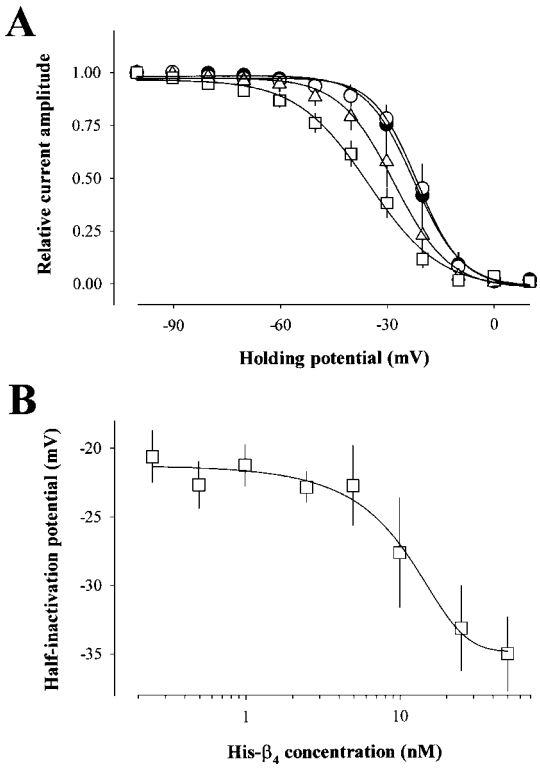

Figure 6 His-β_4 concentration dependence of the shift in voltage-dependent steady-state inactivation

(**A**) Average representative voltage-dependent inactivation curves of $Ca_v2.1$ channels in the absence (●) and presence of His-β_4 (○, 1 nM; △,10 nM; □, 50 nM), illustrating the concentration dependence of the hyperpolarizing shift. $n = 3$–5 cells used for each curve. Average half-inactivation potentials are -22.5 ± 3.4 mV (no His-β_4), -21.3 ± 1.5 mV (1 nM His-β_4), -27.7 ± 6.9 mV (10 nM His-β_4), and -35.1 ± 2.7 mV (50 nM His-β_4). (**B**) Average half-inactivation potential of $Ca_v2.1$ for each His-β_4 concentration. A sigmoidal fit of the data yields a half-effect at a concentration of His-β_4 of 8.8 ± 4.2 nM, and a slope of -6.6 ± 3.3 mV.

GST was immobilized on the matrix demonstrating that it did not contribute significantly to the non-specific binding of His-β_4 on the matrix (results not shown). For the following experiments, we systematically included spermine for the evaluation of His-β_4 binding on GST-$AID_{2.1}$. Next, purified GST and GST-$AID_{2.1}$ fusion proteins were used for the evaluation of His-β_4 binding. Application of 16 nM His-β_4 on GST produces a characteristic bulk response, possibly due to the refraction index of the protein, and which is incremented by a very small non-specific component (Figure 3B). In contrast, application of 16 nM His-β_4 on GST-$AID_{2.1}$ produces a much larger response that includes the bulk response, the non-specific and the specific interactions. The specific His-β_4 binding resulting from the interaction with GST-$AID_{2.1}$ can easily be visualized by a simple subtraction procedure. The interaction between His-β_4 and GST-$AID_{2.1}$ is reversible, a result that accords with two recent studies examining this question, one of which was also performed by SPR [28,29]. It is also consistent with the proposal that in heterologous expression systems, the calcium-channel β subunit would be able to unbind the Ca_v subunit [30]. Evaluation of the specific binding of various His-β_4 protein concentrations on GST-$AID_{2.1}$ allows the calculation of the rate constants of association and dissociation. Figure 3(C) shows the result of a typical analysis. Using the global-fitting method, described by Karlsson and Fält [22], we obtained $k_{on} = 4.1 \times 10^5\ M^{-1} \cdot s^{-1}$ and $k_{off} = 4.5 \times 10^{-3}\ s^{-1}$, and determined a dissociation constant of 10.8 nM for the binding of His-β_4 on GST-$AID_{2.1}$. From three separate experiments, we obtained mean values of k_{on}, k_{off} and K_d as $5.7 \times 10^5\ M^{-1} \cdot s^{-1}$, $5.33 \times 10^{-3}\ s^{-1}$ and 9.3 nM, respectively. The calculated K_d value is thus in strong agreement with earlier calculations based on the use of *in vitro*-translated β_4 subunit and GST-$AID_{2.1}$ fusion proteins immobilized on glutathione beads [20]. These SPR data suggest that the purified His-β_4 subunit has the proper conformation for binding on the AID sequence. In a separate set of experiments, we took advantage of the availability of purified His-β_4, and the capability of the SPR technique to assess protein binding on lipids, to test whether His-β_4 could associate with lipids. These experiments demonstrate that His-β_4 does not bind on phosphatidylcholine or phosphatidylserine (results not shown).

Purified His-β_4 protein has similar functional properties to β_4 protein produced by cRNA injection in *Xenopus* oocytes

The ability of the purified His-β_4 to interact with GST-$AID_{2.1}$ strongly indicates that it may also bind on to the full-length Ca_v channel. To demonstrate this point, we compared the biophysical properties of $Ca_v2.1$ channels expressed in *Xenopus* oocytes after injection of $Ca_v2.1$ cRNA alone [19] or in combination with purified His-β_4 subunit or β_4 cRNA (β_{4RNA}, β_4 expressed by cRNA injection). If the purified His-β_4 protein has a conformation similar to the native β_4 subunit, it should be able to mimic several of the regulatory properties produced by β_{4RNA}. Figure 4(A) demonstrates that the His-β_4 protein indeed has

properties indistinguishable from the β_4 subunit produced by cRNA injection into the *Xenopus* oocytes. As in the case of $\beta_{4\,RNA}$, the recombinant His-β_4 increases the expression level of $Ca_v2.1$ in *Xenopus* oocytes significantly (Figure 4B). At a membrane potential of 20 mV, we observed an average Ba^{2+} current density of 0.42 ± 0.18 $\mu A/\mu F$ ($n = 7$) for $Ca_v2.1$ channels expressed alone, whereas the current densities for $Ca_v2.1/\beta_{4\,RNA}$ and $Ca_v2.1$/His-β_4 were 3.83 ± 1.86 $\mu A/\mu F$ ($n = 7$) and 3.66 ± 1.76 $\mu A/\mu F$ ($n = 9$), respectively. The total β_4-induced increase in current density was therefore 9.1- and 8.7-fold for $\beta_{4\,RNA}$ and His-β_4, respectively. The His-β_4 protein also conserved the ability to produce the characteristic displacements in voltage dependence of activation (Figure 4C) and inactivation (Figure 4D). The half-activation potential measured for $Ca_v2.1$/His-β_4 (-5.1 ± 1.3 mV, $n = 11$) is in close agreement with that of $Ca_v2.1/\beta_{4\,RNA}$ (-5.0 ± 0.8 mV, $n = 7$). These values thus represent a -8.5 to -8.6 mV shift in the voltage dependence of activation of $Ca_v2.1$ channels, since the half-activation potential measured in the absence of β_4 subunit was 3.5 ± 0.6 mV ($n = 19$; Figure 4C). Also, as for $Ca_v2.1/\beta_{4\,RNA}$ channels, the half-inactivation potentials of $Ca_v2.1$/His-β_4 channels were shifted towards hyperpolarizing potentials compared with $Ca_v2.1$ channels. Half-inactivation potentials were -22.3 ± 0.7 mV ($n = 3$) for $Ca_v2.1$, -44.1 ± 1.6 mV ($n = 7$) for $Ca_v2.1$/His-β_4, and -41.3 ± 0.9 mV ($n = 12$) for $Ca_v2.1/\beta_{4\,RNA}$ (Figure 4D). These data demonstrate that the His-β_4 protein has regulatory properties indistinguishable from those of the β_4 subunit of heterologous origin. These data further illustrate that purified His-β_4 remains active for several days after injection in *Xenopus* oocytes (5–9 days).

Overall, the combined possibilities to inject different concentrations of His-β_4 into oocytes and to observe increases in mean current densities of $Ca_v2.1$, provide a unique opportunity to measure a real binding affinity between the full-length $Ca_v2.1$ channel and the β_4 subunit.

The affinity of His-β_4 for the full-length $Ca_v2.1$ channel expressed in *Xenopus* oocytes is remarkably similar to the affinity of His-β_4 for the AID site *in vitro*

We took advantage of the fact that an important fraction of our purified His-β_4 is able to bind to the $Ca_v2.1$ channel to assess the effect of His-β_4 concentration on the increase in current density. This experiment was also a unique opportunity to evaluate the half-effective His-β_4 concentration required for current increase and thus for association to the full-length $Ca_v2.1$. Figure 5(A) illustrates representative Ba^{2+} current traces elicited at a membrane potential of 20 mV in oocytes expressing $Ca_v2.1$ alone or $Ca_v2.1$ with increasing concentrations of purified His-β_4 protein. The data illustrate that $Ca_v2.1$ current density is slightly enhanced at a His-β_4 concentration of 0.5 nM, whereas a maximal increase is monitored at 50 nM. A mathematical fit for the average data provides an EC_{50} of 7.4 ± 2.5 nM for the increase in current density by His-β_4 protein (Figure 5B). This value is thus in remarkable agreement with the affinity measurements made by SPR, or those published earlier [20], using purified $AID_{2.1}$ fusion proteins, in which we measure dissociation constants of 9 and 2 nM, respectively. They confirm previous studies [8,18] that suggested that the enhancement in channel expression at the plasma membrane fully relies on the I–II loop. These data further suggest for the first time that the AID site is fully accessible to the β subunit in its native environment. In brief, physical or chemical constraints brought into AID by the channel conformation and/or interaction of the I–II loop with other channel sequences [31] or protein partners [32,33] barely influences the accessibility of the site to the β subunit. His-β_4 not only enhances the expression level of $Ca_v2.1$ at the cell surface, but also modifies its voltage dependence (Figure 4). Hence it was anticipated that a similar concentration dependence should be observed for this parameter as well. Figure 6(A) illustrates that increasing concentrations of His-β_4 does indeed produce a progressively greater shift in the voltage dependence of inactivation. The half-inactivation value of $Ca_v2.1$ varies between -22.5 ± 3.4 mV (no His-β_4) and -35.1 ± 2.7 mv (50 nM His-β_4). An estimate of the shift of half-inactivation potential produced by His-β_4 demonstrates that the half-effect on inactivation occurs at a concentration of 8.8 ± 4.2 nM (Figure 6B). This value is thus also in close agreement with the EC_{50} value of 7.4 ± 2.5 nM determined for the current enhancement by His-β_4. These data further demonstrate that the modification in voltage dependence of inactivation strongly relies on the association of His-β_4 with $AID_{2.1}$.

Overall, our data indicate that we successfully purified a calcium-channel protein that has binding and regulatory properties similar to the native β_4 subunit. Indications of the feasibility of such an approach have been suggested by Yamaguchi and coworkers [34], who reported that purified His-β_3 is able to regulate effectively yet another calcium-channel type, $Ca_v1.2$. Here, we extend this observation considerably by many important and some novel contributions. First, we demonstrated that the purified His-β_4 is able to bind to the AID site. This represents an important index of the appropriate folding of the purified protein. Secondly, we developed an efficient SPR-binding assay to investigate the association of the β subunit with its main anchoring and regulatory region on the calcium channel. Thirdly, we demonstrated for the first time that the purified β_4 subunit has the same affinity for the full-length channel as for a fusion protein containing the AID site. This observation confirms that the AID site is the main anchoring site for the β subunit in its native environment. It also strongly suggests that *in vitro* collaborative strategies to design drugs that interfere with the association of β subunit to the AID site are valuable approaches to the short- and long-term regulation of calcium-channel activity.

The ability to purify large amounts of functional β subunits opens up valuable scientific opportunities to aid understanding of the role of this subunit in channel function. Current efforts to obtain a crystal structure of the β_4 subunit should be facilitated. The use of the purified protein should also be of interest in ligand experiments in which protein partners of β_4 could be discovered.

We thank CAPES for fellowship support to A.M. We are indebted to INSERM and CEA for financial support. M.D.W. is supported by an ACI grant from the French Ministry of Research.

REFERENCES

1 Bito, H., Deisseroth, K. and Tsien, R. W. (1997) Ca^{2+}-dependent regulation in neuronal gene expression. Curr. Opin. Neurobiol. **7**, 419–429
2 Augustine, G. J., Charlton, M. P. and Smith, S. J. (1987) Calcium action in synaptic transmitter release. Annu. Rev. Neurosci. **10**, 633–693
3 Ertel, E. A., Campbell, K. P., Harpold, M. M., Hofmann, F., Mori, Y., Perez-Reyes, E., Schwartz, A., Snutch, T. P., Tanabe, T., Birnbaumer, L., Tsien, R. W. and Catterall, W. A. (2000) Nomenclature of voltage-gated calcium channels. Neuron **25**, 533–535
4 Stea, A., Dubel, S. J., Pragnell, M., Leonard, J. P., Campbell, K. P. and Snutch, T. P. (1993) A beta-subunit normalizes the electrophysiological properties of a cloned N-type Ca^{2+} channel alpha 1-subunit. Neuropharmacology **32**, 1103–1116
5 Walker, D. and De Waard, M. (1998) Subunit interaction sites in voltage-dependent Ca^{2+} channels: role in channel function. Trends Neurosci. **21**, 148–154
6 Berrow, N. S., Campbell, V., Fitzgerald, E. M., Brickley, K. and Dolphin, A. C. (1995) Antisense depletion of beta-subunits modulates the biophysical and pharmacological properties of neuronal calcium channels. J. Physiol. (Cambridge) **482**, 481–491

7 Gregg, R. G., Messing, A., Strube, C., Beurg, M., Moss, R., Behan, M., Sukhareva, M., Haynes, S., Powell, J. A., Coronado, R. and Powers, P. A. (1996) Absence of the beta subunit (cchb1) of the skeletal muscle dihydropyridine receptor alters expression of the alpha(1) subunit and eliminates excitation–contraction coupling. Proc. Natl. Acad. Sci. U.S.A. **93**, 13961–13966

8 Bichet, D., Cornet, V., Geib, S., Carlier, E., Volsen, S., Hoshi, T., Mori, Y. and De Waard, M. (2000) The I–II loop of the Ca^{2+} channel α_1 subunit contains an endoplasmic reticulum signal antagonized by the β subunit. Neuron **25**, 177–190

9 Isom, L. L., De Jongh, K. S. and Catterall, W. A. (1994) Auxiliary subunits of voltage-gated ion channels. Neuron **12**, 1183–1194

10 Brice, N. L. and Dolphin, A. C. (1999) Differential plasma membrane targeting of voltage-dependent calcium channel subunits expressed in a polarized epithelial cell line. J. Physiol. (Cambridge) **515**, 685–694

11 Beguin, P., Nagashima, K., Gonoi, T., Shibasaki, T., Takahashi, K., Kashima, Y., Ozaki, N., Geering, T., Iwanaga, T. and Seino, S. (2001) Regulation of Ca^{2+} channel expression at the cell surface by the small G-protein kir/Gem. Nature (London) **411**, 701–706

12 Hanlon, M. R., Berrow, N. S., Dolphin, A. C. and Wallace, B. A. (1999) Modelling of a voltage-dependent Ca^{2+} channel beta subunit as a basis for understanding its functional properties. FEBS Lett. **445**, 366–370

13 Burgess, D. L., Jones, J. M., Meisler, M. H. and Noebels, J. L. (1997) Mutation of the Ca^{2+} channel beta subunit gene Cchb4 is associated with ataxia and seizures in the lethargic (lh) mouse. Cell **88**, 385–392

14 Escayg, A., De Waard, M., Lee, D. D., Bichet, D., Wolf, P., Mayer, T., Johnston, J., Baloh, R., Sander, T. and Meisler, M. H. (2000) Coding and noncoding variation of the human calcium-channel beta4-subunit gene CACNB4 in patients with idiopathic generalized epilepsy and episodic ataxia. Am. J. Hum. Genet. **66**, 1531–1539

15 Chien, A. J., Carr, K. M., Shirokov, R. E., Rios, E. and Hosey, M. M. (1996) Identification of palmitoylation sites within the L-type calcium channel beta(2a) subunit and effects on channel function. J. Biol. Chem. **271**, 26465–26468

16 Bogdanov, Y., Brice, N. L., Canti, C., Page, K. M., Li, M., Volsen, S. G. and Dolphin, A. C. (2000) Acidic motif responsible for plasma membrane association of the voltage-dependent calcium channel beta1b subunit. Eur. J. Neurosci. **12**, 894–902

17 Arnaud, N., Cheynet, V., Oriol, G., Mandrand, B. and Mallet, F. (1997) Construction and expression of a modular gene encoding bacteriophage T7 RNA polymerase. Gene **199**, 149–156

18 Pragnell, M., De Waard, M., Mori, Y., Tanabe, T., Snutch, T. P. and Campbell, K. P. (1994) Calcium channel beta-subunit binds to a conserved motif in the I–II cytoplasmic linker of the alpha 1-subunit. Nature (London) **368**, 67–70

19 Mori, Y., Friedrich, T., Kim, M.-S., Mikami, A., Nakai, J., Ruth, P., Bosse, E., Hofmann, F., Flockerzi, V., Furuichi, T., Mikoshiba, K., Imoto, K., Tanabe, T. and Numa, S. (1991) Primary structure and functional expression from complementary DNA of a brain calcium channel. Nature (London) **350**, 398–402

20 De Waard, M., Witcher, D. R., Pragnell, M., Liu, H. and Campbell, K. P. (1995) Properties of the alpha1-beta anchoring site in voltage-dependent Ca^{2+} channels. J. Biol. Chem. **270**, 12056–12064

21 Geib, S., Sandoz, G., Carlier, E., Cornet, V., Cheynet-Sauvion, V. and De Waard, M. (2001) A novel *Xenopus* oocyte expression system based on cytoplasmic coinjection of T7-driven plasmids and purified T7-RNA polymerase. Recept. Channels **7**, 331–343

22 Karlsson, R. and Fält, A. (1997) Experimental design for the kinetic analysis of protein–protein interactions with surface plasmon resonance biosensors. J. Immunol. Methods **200**, 121–133

23 De Waard, M. and Campbell, K. P. (1995) Subunit regulation of the neuronal alpha1A Ca^{2+} channel expressed in *Xenopus* oocytes. J. Physiol. (Cambridge) **485**, 619–634

24 Eppig, J. J. and Dumont, J. N. (1976) Defined nutrient medium for the *in vitro* maintenance of *Xenopus laevis* oocytes. In Vitro **12**, 418–427

25 Marquart, A. and Flockerzi, V. (1997) Alpha(1)-beta interaction in voltage-gated cardiac L-type calcium channels. FEBS Lett. **407**, 137–140

26 Danelian, E., Karlén, A., Karlsson, R., Winiwarter, S., Hansson, A., Löfas, S., Lennernäs, H. and Hämäläinen, M. D. (2000) SPR biosensor studies of the direct interaction between 27 drugs and a liposome surface: correlation with fraction absorbed in humans. J. Med. Chem. **43**, 2083–2086

27 Myszka, D. G. and Rebecca, L. R. (2000) Implementing surface plasmon resonance biosensors in drug discovery. PSTT **3**, 310–317

28 Bichet, D., Lecomte, C., Sabatier, J. M., Felix, R. and De Waard, M. (2000) Reversibility of the Ca(2+) channel alpha(1)-beta subunit interaction. Biochem. Biophys. Res. Comm. **277**, 729–735

29 Canti, C., Davies, A., Berrow, N. S., Butcher, A. J., Page, K. M. and Dolphin, A. C. (2001) Evidence for two concentration-dependent processes for β-subunit effects on α1B calcium channels. Biophys. J. **81**, 1439–1451

30 Restituito, S., Cens, T., Rousset, M. and Charnet, P. (2001) Ca^{2+} channel inactivation heterogeneity reveals physiological unbinding of auxiliary beta subunits. Biophys. J. **81**, 89–96

31 Restituito, S., Cens, T., Barrere, C., Geib, S., De Waard, M. and Charnet, P. (2000) The beta2a subunit is a molecular groom for the Ca^{2+} channel inactivation gate. J. Neurosci. **20**, 9046–9052

32 De Waard, M., Liu, H., Walker, D., Scott, V. E., Gurnett, C. A. and Campbell, K. P. (1997) Direct binding of G-protein $\beta\gamma$complex to voltage-dependent calcium channel. Nature (London) **385**, 446–450

33 Zamponi, G. W., Bourinet, E., Nelson, D., Nargeot, J. and Snutch, T. P. (1997) Crosstalk between G proteins and protein kinase C mediated by the calcium channel alpha1 subunit. Nature (London) **385**, 442–446

34 Yamaguchi, H., Hara, M., Strobeck, M., Fukasawa, K., Schwartz, A. and Varadi, G. (1998) Multiple modulation pathways of calcium channel activity by a beta subunit. Direct evidence of beta subunit participation in membrane trafficking of the alpha1C subunit. J. Biol. Chem. **273**, 19348–19356

Received 15 August 2001/5 February 2002; accepted 1 March 2002